Experimental Investigation on Thermal Efficiency of Indirect Forced Convection Solar Tunnel Dryer

A. Sotoodeh[1]*, A. S. A. Hamid[2], A. Ibrahim[3], K. Sopian[4]

*[1]Ph.d Scholar, Solar Energy Research Institute, Universiti Kebangsaan Malaysia

[2]Faculty of Science and Natural Resources, Universiti Malaysia Sabah, 88400 Kota Kinabalu, Sabah, Malaysia

[3]Research Fellow, Solar Energy Research Institute, Universiti Kebangsaan Malaysia

[4]Professor and Director, Solar Energy Research Institute, Universiti Kebangsaan Malaysia

*Corresponding author: Ali Sotoodeh

Abstract.

This paper aims to evaluate the performance of a small-scale indirect forced convection solar tunnel dryer and more specifically the thermal efficiency of the said dryer. The solar tunnel dryer (STD) which is one of the common types of dryers utilizes sunlight to dry various agricultural products. The STD which is a semi-cylindrical and energy saving dryer is able to operate in remote areas. The performance of solar tunnel dryers depends on different contributing factors such as air convection mode, solar irradiance, ambient temperature and relative humidity, air velocity and load's features. In order to investigate and find the optimum thermal efficiency, variable and constant airflow velocity were tested and their thermal efficiencies were obtained. It was found that, at no-load condition, the maximum thermal efficiency for variable airflow velocity was 26.3 % and for constant 7m/s airflow velocity the figure was 52.4 %. The average absorber inlet and outlet temperature were 32.9 ^{o}C and 62.1 ^{o}C, and relative humidity were 50 % and 27.4 % respectively. The maximum variable air velocity was 6.3 m/s at an irradiance of 886 W/m^2 during the daytime. In addition, the total solar energy available, peak sun hour, and input energy were determined as 5.5 kWh/d, 5.5 h, 19.3 kWh respectively.

Keywords: Thermal energy, solar tunnel dryer, dried fruit, experimental study

1. Introduction

Numerous studies have considered solar energy as the viable and environmentally friendly alternative energy source for future. In addition, this type of energy can be harnessed and utilized with countless applications such as drying. Drying is one of the most essential and practical methods of preserving the shelf life and quality of the agricultural products. Traditionally, agricultural products are dried under direct sunlight. Although this method is simple and inexpensive, it has some drawbacks including non-uniform drying, uncontrollable rate of drying, large area requirement, high chance of deterioration due to environmental and ambient conditions such as rainfall, dust, wind, animals and rodents which lead to poor quality of dried products. To eliminate the above-mentioned drawbacks and improve the quality of dried products and also the cost of energy, solar dryers have become a popular alternative to open sun-drying technique [1-5]. Solar dryers are known to be more efficient, reliable, and energy-saving option compared to other conventional types of drying methods like open sun drying [6-9]. Among various types of solar dryers, solar tunnel dryer is proven to be efficient, trustworthy, simple, and economical. When the load is placed in the drying chamber and exposed to thermal energy, the drying process takes place in two main stages [10-12]. In addition, the optimum design of solar dryers are able to reduce drying duration and effect on yield and drying performance

i. Transfer the internal moisture to the surface of the products due to thermal energy. The percentage of load's moisture content, physical structure such as depth and drying chamber's temperature are influential factors in this stage of the operation.
ii. The heated air in the drying chamber transfers the moisture from the surface of the loads to outside via chimney or exhaust. Airflow temperature, relative humidity, velocity, pressure, and dryer design impact the function of this stage.

The drying process needs to be completed fast enough in order to reduce the losses due to the growth of microorganisms that grow quickly in presence of humidity. This often will affect the quality of the products [13].

The objective of a solar dryer is to increase the moisture absorption capacity of the inlet air. The entrance air is heated as it passes through the thermal collector and the load will be exposed to the heated air. At the output drying chamber, partial heat loss will take place due to absorbing moisture from the products. The higher the temperature of the air is; the more moisture content it absorbs. Therefore, the amount of moisture removal depends on relative humidity and air temperature in the inlet drying chamber [9,12].

As is illustrated in Figure 1. Solar dryers can be categorized in two main types namely natural convection and forced convection [1,8]. Natural convection solar dryers use the ambient airflow and diffuse sunlight to dry products without utilizing any power source such as electric fans [10,14]. The drying rate is slow and highly dependent on ambient conditions that lead to the low quality of the drying products especially in adverse atmospheric conditions [15]. However, the capital and maintenance cost of this type of convection mode is lower than the forced convection [9].

Forced convection mode, which is also known as active convection, utilizes a power source such as DC power supply or PV panel to create adjustable airflow in solar dryers. Since the airflow is controllable, the force convection drying system is able to dry various kinds of loads. This mode of convection is more efficient and reliable. Although the capital cost of this dryer is more than natural convection, the drying process will occur faster [14].

Figure 1: Classification of solar dryer convection mode

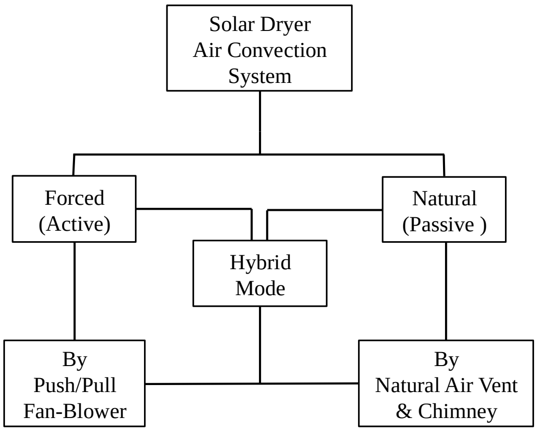

Solar tunnel dryers (STD) typically have forced convention system. Drying tray, collector plate, and a number of fans are the main components of STD. Inlet air that enters the solar tunnel dryers is heated by the absorber. The heated air from the absorber is forced to pass over and through the products placed in the drying chamber and to absorb moisture from them using the fan located at the air inlet of the solar tunnel dryer [15,16]. This fan provides the required flow rate of the air and is connected to solar panels or other source of energy to generate the required power [17]. The air velocity in forced solar dryer is constant, unless change the fan speed. The performance of solar tunnel dryer mainly depends on various parameters such as solar radiation values, airflow velocity, ambient temperature, humidity of inlet air, temperature and humidity of air in contact with the crops, and types of absorber [18].

2. Methodology

The main purpose of this study is to evaluate the performance of the indirect forced convection solar tunnel dryer and thermal efficiency on constant and variable airflow velocity. The solar tunnel dryer that was used in this experimental study was fabricated and tested at solar thermal open-air laboratory site at solar energy research institute (SERI), the National University of Malaysia. The experiment latitude, longitude and altitude are 2.5513 N, 101.4618 E and 44 m above sea level respectively.

2.1 The Solar Tunnel Dryer (STD)

The solar tunnel dryer's airflow convention system is based on forced mode and indirect exposure to insolation. The semi-cylindrical shape STD dimensions are 4.46 m long, 1.22 m wide and 0.8 m height. The Solar tunnel dryer is divided into two sections; fluid terminal section (FTs), and drying chamber section (DCs). The STD schematic is shown in Figure 2. Solar exhaust fan, transmission tubes, and inlet air valve are included in FTs while absorber plate and crops bed trays are included in DCs. The drying chamber section is covered by flexible polycarbonate sheets.

Figure 2: Schematic of indirect forced solar tunnel dryer

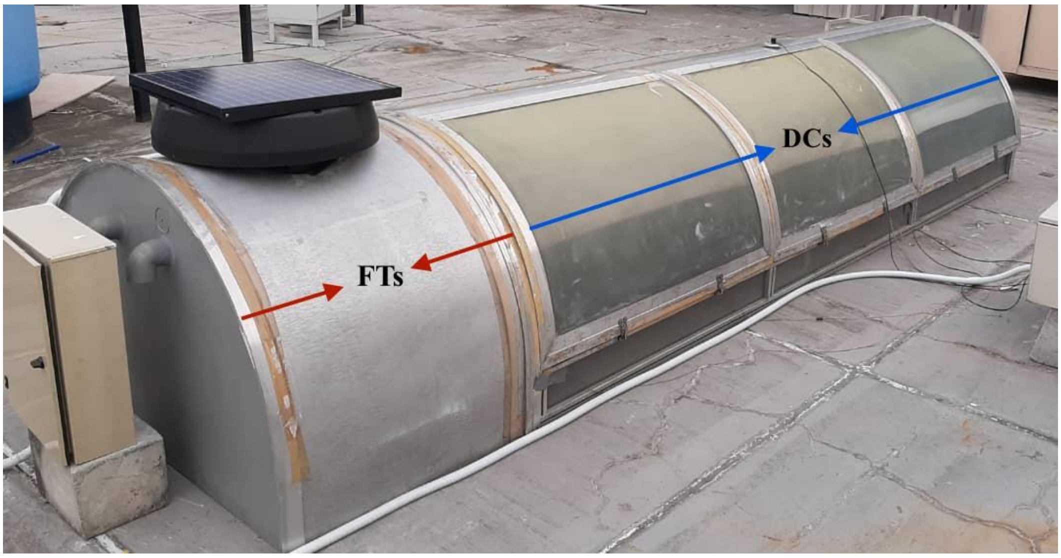

2.2 STD Fluid Operation Method

The dryer's forced air convection system is based on draft convection. The ambient air enters into the inlet thermal absorber area via twin 6 cm diameter steel tubes. The solar radiation incident increases the temperature of the absorber plates. Therefore, when the inlet airflow passes through the absorber, its temperature escalates and relative humidity decreases. At the end of thermal absorber plate, the heated airstream enters trays area. The load on perforated trays will be exposed to the heated air, then the heated airstream carries the load's surface moisture through the bottom channel of the drying chamber and into the exhaust vent. The airflow movement is created by solar exhaust fan. Figure 3. displays the airflow direction and STD inner components and Table 1 explains the solar tunnel dryer components as well as their details.

Table 1: Description of solar dryer components

No.	Component	Description
1	Polycarbonate cover	Transparent polycarbonate glazing with 6 mm thickness allows radiation incident to the thermal absorber also retains heat inside the dryer. In addition, the drying chamber load/unload doors are covered by polycarbonate.
2	Thermal Absorber	The 1mm thickness corrugated thermal absorber sheet is made of steel. The length and width were 3470 mm and 970 mm respectively. The corrugated shape assists the absorber to increase thermal capacity. Absorber was painted in matt black color to reduce reflection and increase absorption.
3	Inlet Air Vale	Airflow enters via two 6 cm diameter circle, the inlet air valve connected to the transmission tube to transfer ambient air to absorber inlet.
4	Load Tray	The load trays were made of aluminium. Three trays were perforated to penetrate the heated airflow into load and then lower channel. Total area of the trays is 4 m^2 and they are elevated 18 cm.
5	Solar exhaust fan (SEF)	The solar photovoltaic and exhaust fan were combined and thus considered as one component. A 40 W mono crystalline PV generates required power for DC fan.
6	Air transmission tubes	The two steel pipes connect dryer inlet air valve to the absorber inlet. The pipes were located at FTs, the length of each tube is 700 mm, and diameter is 60 mm.

Figure 3: Inner components of solar tunnel dryer

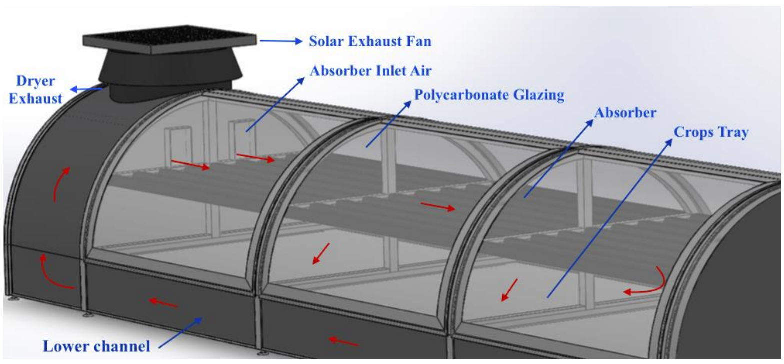

The following Figure 4. Shows the position of thermal absorber plate, load tray and lower channel inside the drying chamber.

Figure 4: Thermal absorber plate, load tray and lower channel

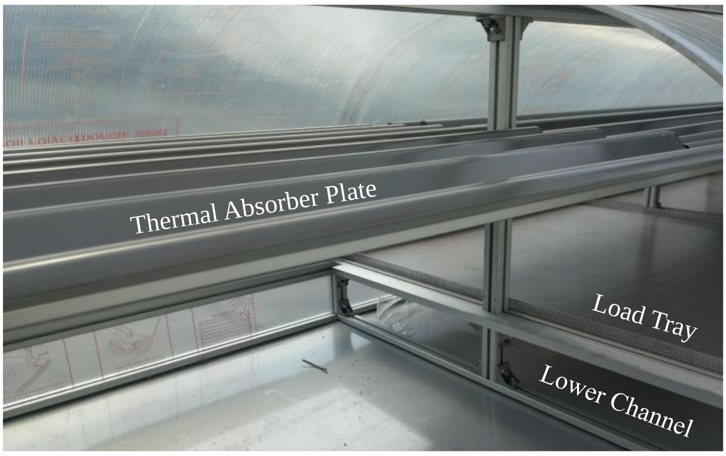

2.3 Convection System

Solar exhaust fan (SEF) as the main component of convection system has an important role to create sufficient air velocity, exhaust the airflow, generate power for the fan, and to determine the dryer mass flow rate ($\dot{m}$). The dryer's forced air convection system is based on draft convection. The SEF includes two circles, the inner circle draws the drying chamber outlet airflow and outer circle sprays the drawn air out from the sides of SEF. However, the fluctuations of fan's revolutions per minute (RPM) and mass flow rate depend on solar irradiance intensity. Therefore, higher irradiance intensity creates higher inlet airflow velocity. The maximum toleration of fan speed is 8.5 m/s. The three blades fan operates with direct current (DC). Figure 5. Shows the parts of solar exhaust fan. Eq. 1 defines the relation between inlet airflow velocity and mass flow rate.

$$\dot{m} = A.V \quad (1)$$

Where,

$\dot{m}$: Mass flow rate

A: Inlet fluid area

V: Fluid velocity

Figure 5: Solar exhaust fan segments

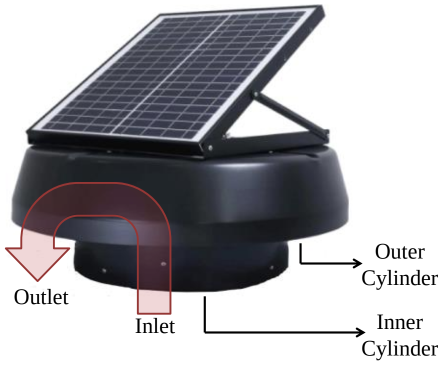

2.4 Convert Variable Mass Flow Rate to Constant Mass Flow Rate

Although the solar dryer inlet air is considered as variable velocity, with a number of changes in SEF, it can also operate as a constant inlet airflow velocity. Figure 6. demonstrates the mass flow rate conversion from variable to constant.

Figure 6: Constant airflow velocity system

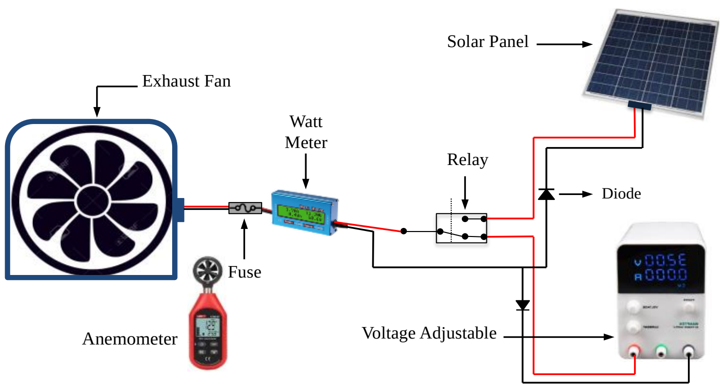

The conversion process involves in five steps: disconnect the photovoltaic panel and exhaust fan, connect the exhaust fan to DC power supply, hold anemometer on inlet valve, increase power supply voltage until the anemometer shows 7meter/second, leave power supply at determined range and run data acquisition.

2.5 Measurement System

In order to record dryer and ambient data, Midi Logger GL820 data acquisition was used. Thermocouples, hygrometers, and pyranometer were connected to data logger directly. Table 2 shows number and specific information about sensors.

Table 2: Parameter specifications

Parameter - Unit	Sensor	Quantity	Type	Accuracy
Temperature - ˚C	Thermocouple	8	K-type, -200 to +1350	± 2.2
R. Humidity - %	Hygrometer	2	B-530	± 2~5
Air velocity - m/s	Anemometer	1	Uni-T UT363BT	± 1
Radiation - W/m^2	Pyranometer	1	Apogee SP-110-ss	0.2 mV

According to Figure 7. The V_i is anemometer which is placed during recording inlet velocity, G_{out} is outside pyranometer, T_{am} and H_{am} represent ambient temperature and relative humidity, T_{ia} and H_{ia} stand for absorber inlet temperature and relative humidity, T_{oa} and H_{oa} are absorber outlet temperature and relative humidity, T_{oe} and H_{oe} are temperature and relative humidity at SEF output. The amount of T_{am} = T_{ia} and H_{am} = H_{ia} and T_{oa} = T_{it} and H_{oa} = H_{it}.

Figure 7: Solar dryer's sensors spots and fluid direction

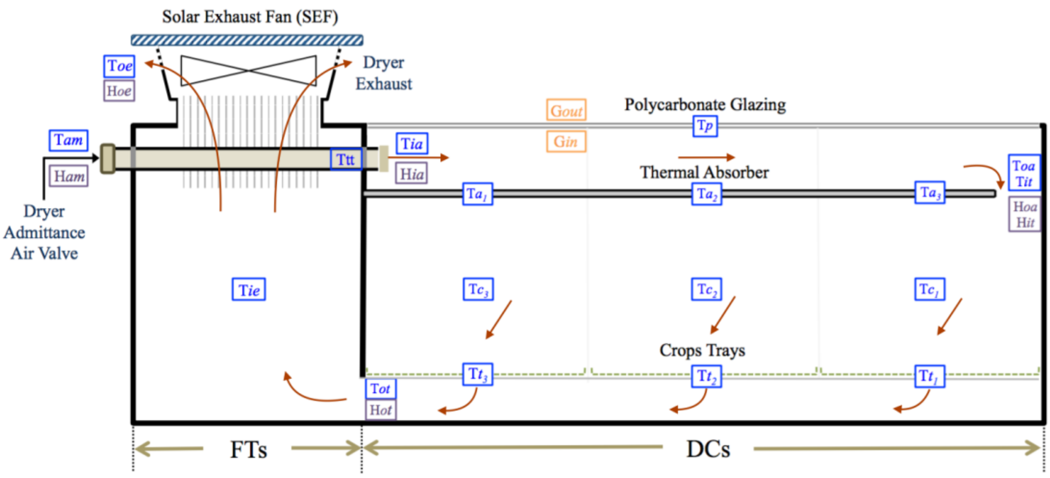

2.6 Solar Tunnel Dryer Evaluation

The experiment took place from 9 a.m. to 7 p.m. to assess and compute the total solar energy, peak sun hours, and compare thermal efficiency at variable inlet air velocity and 7m/s steady inlet air velocity. Solar energy available during testing period was based on irradiance intensity reading. The total solar energy available was calculated by the sum of the average of every hour value as shown in Eq.2 where the Q_{solar} is kWh/d unit.

$$Q_{solar} = (I_2 + I_2 + \cdots + I_L) \tag{2}$$

Where,

I_1: Irradiance intensity for first hour

$I_2 + \cdots$: Irradiance intensity for the second hour and next hours

I_L: Irradiance intensity for the last hour.

The peak sun hour (PSH), which represents the number of hours the solar irradiance intensity reaches an average of 1000 watts/meter2, is calculated by total solar energy over 1000. The (PSH) is expressed by Eq.3:

$$PSH = \frac{Q_{solar}}{1000} \tag{3}$$

The amount of solar energy reaches to the absorber is calculated by considering irradiance intensity times absorber area. This is the input energy of the dryer and is determined by using Eq. 4. The unit is kWh/d.

$$Q_{in} = (AI_2 + AI_2 + \cdots + AI_L) \tag{4}$$

Where,
A: Absorber area
To evaluate the thermal efficiency of the absorber Q_{in} and Q_{out} are the required date. Thermal efficiency can be calculated by Q_{out} over Q_{in}. which is shown in Eq. 5:

$$\mu_{th} = \frac{Q_{out}}{Q_{in}} = \frac{\dot{m}C(T_o - T_i)}{AI} \tag{5}$$

Where,
C: Specific heat capacity ($kg^{-1}.\ k^{-1}$)
T_o: Outlet absorber temperature (˚C)
Ti: Inlet absorber temperature (˚C)
Loading density refers to the amount of the crops loaded on the area of trays. Loading density is calculated mathematically as follow:

$$LD = \frac{W_{Fresh\ Produc}}{A_d} \tag{6}$$

Where,
LD: Loading Density
$W_{fresh\ product}$: Fresh product weight (kg)
A_d: Area of trays (m^2)

3. Results and Discussions

The air temperature, air relative humidity, air velocity and solar radiation are the contributing factors to evaluate the performance of solar tunnel dryers. The temperature trends are plotted in Figure 8. The ambient temperature, which is equivalent to absorber inlet temperature ranges between 28˚C to 36.2˚C. The minimum and maximum airflow temperature after passing through the absorber are 39.2˚C and 80˚C. The average temperature difference between inlet and outlet of absorber is 30˚C. The results revealed a direct correlation between irradiance and the outlet temperature. Solar radiation uptrend started from 305 W/m2 at 9:00 a.m. to 866 W/m2 at 1:00 p.m. The absorber outlet temperature and solar irradiance intensity experienced an almost similar pattern.

Figure 8: Variation of air temperature under no-load condition

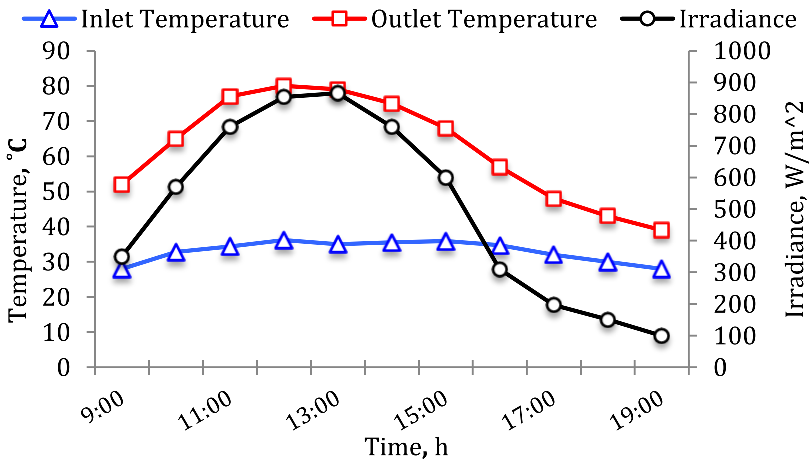

The relative humidity is illustrated in Figure 9. As it can be seen, there is an inverse relationship between the irradiance and relative humidity. The minimum and maximum relative humidity from 9 a.m. to 7 p.m. were 19% and 43% for inside the drying chamber and 43%, 60% for the ambient. Average percent of airflow RH was recorded 50.2% before and 27.4% after thermal absorber. The maximum difference between inside and outside humidity of the dryer was 28% which occurred at 3 p.m. In addition, the lowest inside relative humidity was also recorded at 3 p.m. with 19%. While the solar irradiance was 866 W/m^2 (maximum intensity), the ambient RH reduced by 23%. These outcomes confirmed the effective moisture removal capability of this solar tunnel dryer. Outside humidity equals to ambient humidity and absorber inlet humidity, and inside humidity equals to outlet absorber humidity.

Figure 9: Variation of air relative humidity under no-load condition

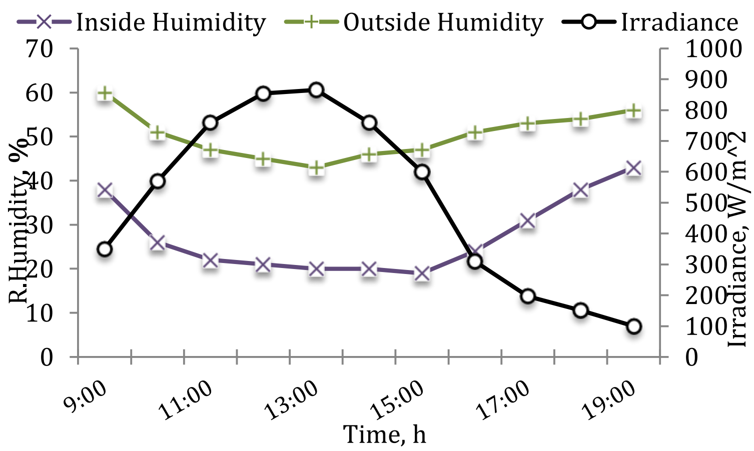

Figure 10. Illustrates the variation of airflow velocity and irradiance. The exhaust fan operates by the solar panel and its speed has direct correlation with the irradiance intensity. The air velocity fluctuated between 2.9 m/s and 6.3 m/s during the

experiment. Irradiance peaked at 886 W/m^2 at maximum obtained air velocity. It is obvious that the higher solar radiation leads to increased airflow velocity, which can result in higher thermal efficiency. Air velocity and irradiance followed a similar pattern peaking at 1 p.m. and reaching the lowest point at the end of the experiment.

Figure 10: Variation of air velocity under no-load condition

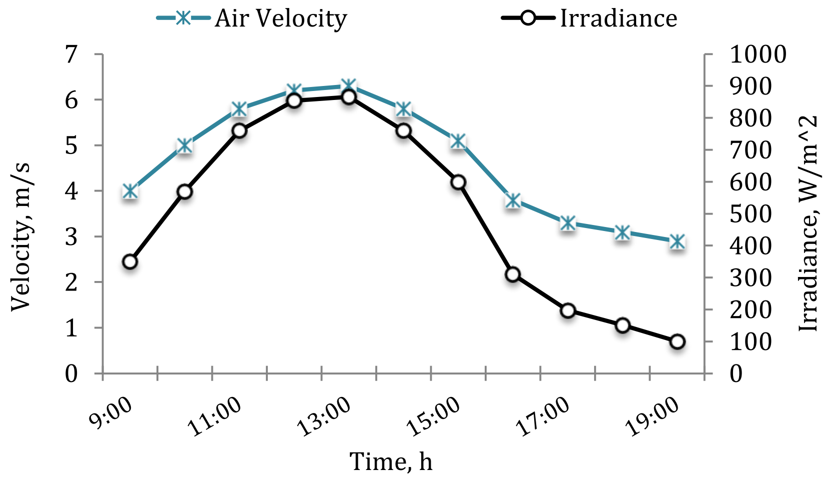

Table 3 shows the airflow velocity rate at different solar irradiance. In this case study, the maximum solar irradiance was 886 W/m2. The table also indicates the projection of air velocity at higher solar irradiance. The predicted air velocity at higher irradiance will be calculated using the Eq.7.

$$\text{Predicted Velocity: } 0.0044 * \text{irradiance} + 2.5206 \quad (7)$$

Table 3: Predicted Dryer air velocity at different solar radiation

Solar Irradiance Intensity (W/m^2)	100	200	300	400	500	600	700	800	900	1000	1100	1200
Inlet Air Velocity (m/s)	2.9	3.4	3.8	4.2	4.7	5.1	5.6	6	6.4	6.9	7.3	7.8

Figure 11. Displays the solar irradiance intensity of each hour during the experiment period. Each column demonstrates the average of radiation value of its hour. The value of Q_{solar} was calculated as 5.5 kWh/d. Eq. 3 was used to determine peak sun hour (PSH) which was 5.5 h. The input energy was computed by using Eq. 4. Total energy input was 19.3 kWh.

Figure 11: Hourly average solar radiation available during experiment period

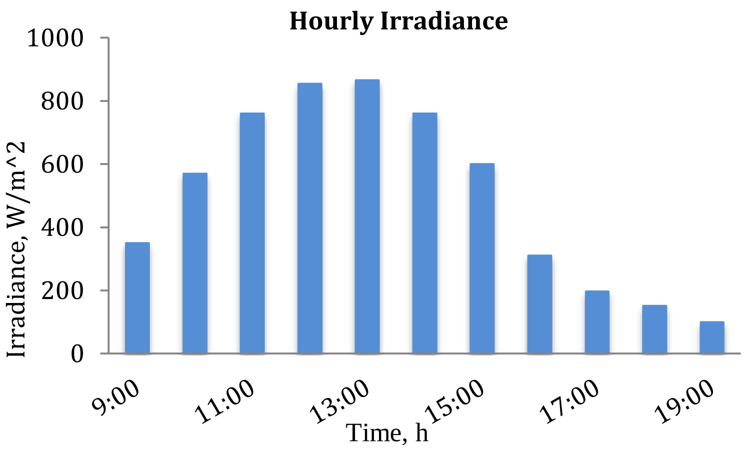

The thermal efficiencies of variable airflow velocity and constant airflow velocity of the solar tunnel dryer which were calculated by Eq. 5 are shown in the Figure 12. The average thermal efficiency in constant 7 m/s is higher than the variable one. The average thermal efficiency for variable and constant airflow velocity were 23.7 % and 37.1 % respectively.

Figure 12: Solar thermal efficiencies

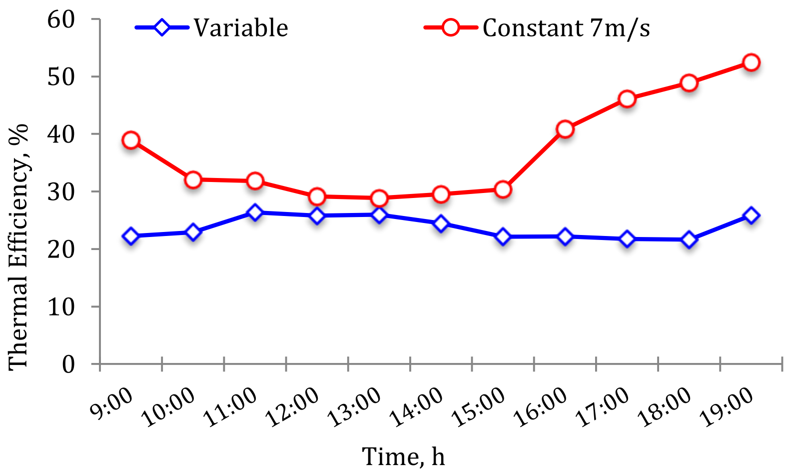

3. Conclusion

The forced convection solar tunnel dryer was fabricated and tested at the Solar Energy Research Institute (SERI), Universiti Kebangsaan Malaysia, Bangi, Malaysia. The no-load performance tests were carried out from 9.00 a.m. to 7.00 p.m. on 20/8/2019. The maximum thermal efficiency was reported 26.3 % for variable velocity and 52.4 % for constant 7 m/s velocity, and their average of thermal efficiencies were 23.7 % and 37.1 % respectively. It was observed that thermal efficiency fluctuated continuously due to the changes in variables such as irradiance, velocity and temperature. The proposed solar tunnel dryer was capable to decrease the ambient relative humidity by approximately 13 % to 28 %. The thermal absorber increased the inlet temperature between 11 ˚C and 44 ˚C. The highest temperature was measured at 80 ˚C within the dryer during the experiment. In addition, the variation of air velocity and solar radiation had similar patterns. Air velocity peaked at 6.3 m/s at the summit of irradiance at 886 W/m^2.

Acknowledgment

Authors would like to acknowledge:

- FRGS/1/2019/TK07/UKM/02/4 Skim Geran Penyelidikan Fundamental (FRGS)
- Solar Energy Research Institute, Universiti Kebangsaan Malaysia for providing facilities and technical support.

Reference.

[1]. B. K. Bala and N. Debnath, (2012), *Solar Drying Technology: Potentials and Developments*. Journal of Fundamentals of Renewable Energy and Applications, 21-5.

[2]. G. Tiwaria, V. K. Katiyara, V. Dwivedia, A. K. Katiyarb and C. K. Pandey, (2013). *A Comparative study of commonly used Solar Dryers in India*. International Journal of Current Engineering and Technology, 3994-999.

[3]. B. Paul and S. P. Singh, (2013). *A Review of Solar Dryers Designed and Developed for Chili*. International Journal of Research in Advent Technology, 1, 62-72.

[4]. A. Tiwari, (2016). *A Review on Solar Drying of Agricultural Produce*. Journal of Food Processing and Technology, 7, 1-12.

[5]. U. Toshniwal and S.R. Karale, (2013). *A review paper on Solar Dryer*. International Journal of Engineering Research and Applications, 3, 896-902.

[6]. A Bharathkumar, S L Jagadeesh, Netravati, V Hegde, G Bhuvaneshwari and H Bindu, (2018). *A study on fruit preparation on quality of fig fruits (cv. Bellary) osmotic-dehydrated under solar tunnel dryer*. Journal of Pharmacognosy and Phytochemistry, 7, 3177-3180.

[7]. S. K. Sansaniwal and M. Kumar, (2015). *Analysis of ginger drying inside a natural convection indirect solar dryer: An experimental study*. Journal of Mechanical Engineering and Sciences, 9, 1671-1685.

[8]. M Gavhale, S Kawale, R Nagpure, V.N.Mujbaile, N.S.Sawarkar, (2015). *Design and Development of Solar Seed Dryer*. International Journal of Innovative Science, Engineering and Technology, 2, 1005-1110.

[9]. M. S. Seveda, (2013). *Design of a Photovoltaic Powered Forced Convection Solar Dryer in NEH Region of India*. International Journal of Renewable Energy Research IJRER, 3, 906-912

[10]. I. N. Simate and S. Cherotich. Design and Testing of a Natural Convection Solar Tunnel Dryer for Mango. Journal of Solar Energy, 2017, 1-10.

[11]. M.A. Basunia, H.H. Handali, M.I. Al-Balushi, M.S. Rahman, O. Mahgoub, (2010). *Drying of Dates in Oman Using a Solar Tunnel Dryer*. XVIIthWorld Congress of the International Commission of Agricultural and Biosystems Engineering (CIGR), 1-10.

[12]. N. Karunaraja, P. Prabhakaran, S. Ayyappan and V.V. Sreenarayanan, (2015). *Fabrication and Experimental Analysis of Solar Tunnel Dryer using Thermal Storage Materials*. International Journal for Scientific Research and Development, 3523-526.

[13]. Arjoo, Yadvika and Y.K. Yadav, (2017). *Performance Evaluation of Solar Tunnel Dryer for Drying of Garlic*. Current Agriculture Research Journal, 5, 220-226.

[14]. S. Kumar Singh, P.B.L Chaurasia, H.K. Singh, H. Singh, A Kumar, (2014). *Study of Design Parameters of Solar Dryer for Drying Agriculture Product*. International Journal of Science, Engineering and Technology, 2, 974-986.

[15]. S. Amin, (2008). *Investigation on the Performance of Solar Tunnel Dryer during Rainy Season for Cocoa Beans Drying*. International Energy Journal, 9, 47-52.

[16]. A. Derbala, N.A. Udroiu, A. Mitroi and C. Iacomi, (2009*). Drying of Squash Using Solar Tunnel Dryer with Photovoltaic.* Process Engineering, 26, 922-934.

[17]. B. K. Bala and M. R. A. Mondol, (2001). *Experimental Investigation on Solar Drying of Fish Using Solar Tunnel Dryer*. Drying Technology, 19, 427-436.

[18]. A. S. A. Hamid, A. Ibrahim, S. Mat, K. Sopian, (2019). *Experimental Evaluation on Large Scale Solar Dryer for Drying Natural Fiber in Malaysia.* International Journal of Renewable Energy Research IJRER. Vol.9 No.2.